

Lattice Landau gauge with stochastic quantisation

Jan M. Pawłowski,^{1,2} Daniel Spielmann,^{1,2} and Ion-Olimpiu Stamatescu^{1,3}

¹*Institut für Theoretische Physik, Universität Heidelberg,
Philosophenweg 16, D-69120 Heidelberg, Germany*

²*Extreme Matter Institute EMMI, GSI Helmholtzzentrum für
Schwerionenforschung GmbH, Planckstr. 1, D-64291 Darmstadt, Germany*

³*FEST, Schmeilweg 5, D-69118 Heidelberg, Germany*

We calculate Landau gauge ghost and gluon propagators in pure $SU(2)$ lattice gauge theory in two, three and four dimensions. The gauge fixing method we use, sc. stochastic quantisation, serves as a viable alternative approach to standard gauge fixing algorithms. We also investigate the spectrum of the Faddeev-Popov operator. At insufficiently accurate gauge fixing, we find evidence that stochastic quantisation samples configurations close to the Gribov horizon. Standard gauge fixing does so only at specific parameters; otherwise, there is a clear difference. However, this difference disappears if the gauge is fixed to sufficient accuracy. In this case, we confirm previous lattice results for the gluon and ghost propagator in two, three and four dimensions.

PACS numbers: 12.38.Gc, 05.10.Gg, 11.15.Ha, 12.38.Aw

I. INTRODUCTION

Confinement is one of the key properties of QCD, but its explanation from first principles still remains to be found. While a linearly rising heavy quark-antiquark potential is readily simulated on the lattice, evidence for or against the candidates for the underlying confinement mechanism is more elusive. Some prominent confinement scenarios involve topological defects, like magnetic monopoles or center vortices, and are best described in specific gauges amiable towards the definition of the related defects. It is this gauge dependence which makes it so difficult to pin down the confinement mechanism. There is some evidence that such scenarios are compatible with approaches like the Gribov-Zwanziger scenario [1, 2, 3], according to which configurations in the vicinity of the Gribov horizon account for confinement. This scenario makes specific predictions for QCD's Green's functions, e.g. in Landau gauge that the gluon propagator vanishes in the infrared (IR), the horizon condition. In turn the ghost dressing function is IR divergent, called ghost enhancement. The Kugo-Ojima scenario [4] has similar implications. It aims at describing confinement by the BRST quartet mechanism and requires well-defined global BRST charges. Both scenarios put restrictions on the infrared behaviour of ghost and gluon propagators if confinement is present in the theory. In turn it has been shown recently that ghost and gluon propagators with a sufficiently large IR suppression of the gluon and an IR enhancement of the ghost lead to quark confinement indicated by center symmetry [5]. The related IR suppression of the gluon propagator has been seen in both, lattice studies and continuum approaches, see e.g. [6, 7].

The quantities relevant for such confinement scenarios, like the aforementioned Green's functions, depend on the chosen gauge. Hence these investigations are complicated by the Gribov problem. This problem relates to the fact that local gauge conditions do not single out a unique

gauge copy [1, 8], but allow for an abundance of Gribov copies satisfying the gauge condition on the same gauge orbit.

Interestingly, Landau gauge seems not to fix uniquely the infrared behaviour of the propagators. In continuum computations with functional methods such as Dyson-Schwinger equations (DSE) and functional RG flows one observes a one-parameter family of solutions. The free parameter can be linked to the zero momentum value of the gluon propagator in the infinite volume limit, see [6]. It is suggestive to relate this parameter to global properties of the gauge fixing as Landau gauge still has remnant gauge degrees of freedoms. In the continuum, this infrared boundary condition is implemented by specifying a non-perturbative renormalisation condition, see [6]. It has been demonstrated recently that a corresponding freedom exists also on a finite lattice, and that it is directly connected to the non-perturbative completion of the Landau gauge condition, [9]. Indications for this freedom have already been seen in the strong coupling limit [10, 11, 12] where the effect is rather dramatic [13]. This high sensitivity of the results to the global details of the gauge fixing, in particular for the ghost propagator, calls for a systematic evaluation of the details of the thermodynamical limit of Landau gauge fixings on the lattice. In particular the question of whether the Gribov-Zwanziger scenario is indeed implemented within specific gauge fixings is of importance.

In the present work, we compute ghost and gluon propagators in Landau gauge Yang-Mills theory on the lattice within stochastic quantisation [14, 15, 16], an alternative to standard Monte Carlo simulations. It has recently also received renewed interest e.g. for simulations at finite density [17, 18] or in real time [19]. Here, we employ stochastic quantisation for gauge fixing [20, 21, 22, 23, 24, 25, 26, 27, 28]. In such an approach, a gauge fixing force drives the Langevin evolution towards the first Gribov region. This potentially opens new possibilities to circumvent the Gribov problem. It also fur-

thers the insights and allows for a better understanding of the underlying structures. At insufficiently accurate gauge fixing, we find evidence that stochastic quantisation samples configurations close to the Gribov horizon. Standard gauge fixing does so only for specific parameter choices; otherwise, there is a clear difference. While this difference disappears if the gauge is fixed to sufficient accuracy, the sampling close to the Gribov horizon makes it unlikely that stochastic gauge fixing systematically suppresses contributions from the Gribov horizon. Such a suppression would have the potential of invalidating the argument that in the thermodynamical limit only configurations at the Gribov horizon matter. In summary, our analysis provides strong evidence against one of the reasons for a failure of lattice gauge fixings to reproduce the Gribov-Zwanziger scenario.

In the second section we define ghost and gluon propagators and discuss their general scaling properties. In the third section we introduce our implementation for stochastic quantisation and stochastic gauge fixing. Some of the intricacies of such an approach are then illustrated within a simple finite-dimensional model in the fourth section. In the fifth section we present and discuss our results on ghost and gluon propagators in two, three and four dimensions, which we supplement in the subsequent section with some results on the spectrum of the Faddeev-Popov operator. We close with a short summary and discussion of our results.

II. INFRARED BEHAVIOUR OF THE GHOST AND GLUON PROPAGATOR

We are interested in the infrared behaviour of Green's functions in Landau gauge Yang-Mills theory. Landau gauge is defined via the condition,

$$\partial_\mu A_\mu^a = 0, \quad (1)$$

which is subject to the Gribov ambiguity. In Landau gauge, the gluon and ghost propagator have the form

$$(D_{\text{gl}})_{\mu\nu}^{ab} = \delta^{ab} \left(\delta_{\mu\nu} - \frac{q_\mu q_\nu}{q^2} \right) D_{\text{gl}}(q^2), \quad (2)$$

$$(D_{\text{gh}})^{ab} = -\delta^{ab} D_{\text{gh}}(q^2), \quad (3)$$

they are parametrised by the two scalar functions $D_{\text{gl/gh}}(q^2)$. The standard dressing functions are given by $q^2 D_{\text{gl/gh}}(q^2)$. Functional methods in the continuum such as DSE [29, 30, 31, 32, 33, 34, 35, 36], stochastic quantisation [3, 37, 38] and the functional renormalisation group [6, 39, 40, 41, 42, 43] allow for a scaling solution which is unique [44, 45, 46] and in line with global BRST-symmetry [6, 7, 47]. As mentioned in the introduction, there are strong arguments for a one-parameter family of decoupling solutions where scaling is violated, see [6, 9, 48, 49, 50, 51, 52, 53, 54, 55, 56, 57, 58, 59, 60, 61, 62, 63, 64] for related work. The unique scaling solution is indeed the scaling endpoint of this one-parameter

family, and the corresponding propagators obey power laws in the infrared,

$$\lim_{q^2 \rightarrow 0} D_{\text{gl/gh}}(q^2) \sim \frac{1}{(q^2)^{\kappa_{A/C}+1}}. \quad (4)$$

In $d = 4$ dimensions, the exponents satisfy the scaling relation

$$\kappa_A = -2\kappa_C. \quad (5)$$

It stems from non-renormalisation of the ghost-gluon-vertex [65], which has been confirmed on the lattice [66, 67] as well as from DSE [68]. When varying d , (5) generalises to

$$\kappa_A = -2\kappa_C + (d-4)/2. \quad (6)$$

Assuming a bare ghost-gluon vertex, the predicted values for κ_C , which is also referred to simply as κ , are $\kappa = \frac{1}{98} (93 - \sqrt{1201}) \approx 0.6$ in $d = 4$, $\kappa \approx 0.4$ in $d = 3$ and $\kappa = 0.2$ in $d = 2$ [31].

The aforementioned decoupling solutions imply that both the gluon propagator and the ghost dressing function are finite in the infrared. In contrast to the scaling solution, the decoupling solutions seem to be incompatible with global BRST invariance [6], see [7, 69, 70] for progress towards a lattice BRST formulation. Nevertheless, both solutions exhibit confinement, as both satisfy the confinement criterion put forward in [5] and both lead to positivity violation for the gluon. Positivity violation has been explicitly confirmed on the lattice in $d = 3$ [71] and $d = 4$ [72, 73] and also from DSE [74].

A. Lattice simulations in $d = 2, 3, 4$

Lattice simulations have so far found no clear evidence of a scaling behaviour, with the possible exception of the two-dimensional case [75, 76], which lacks dynamics [77]. Very recently it has been shown that the scaling behaviour might also be absent in two dimensions for the lattice Landau gauge fixings used so far [13]. In four dimensions, lattice simulations of $SU(2)$ or $SU(3)$ [72, 76, 78, 79, 80, 81, 82, 83] yield an IR finite gluon propagator even on volumes up to $(27 \text{ fm})^4$. DSE studies on a torus suggest that this volume could suffice for the correct infinite volume behaviour to be visible [84]. While dissenting results concerning IR finiteness exist [85, 86, 87, 88], they tend to yield an IR exponent closer to $\kappa = 0.5$, implying an IR finite propagator, than to the predicted value of ≈ 0.6 .

Also for $d = 3$, lattice results clearly favour decoupling, e.g. [89], even at $(85 \text{ fm})^3$ [80]. Recently, following a discussion of non-perturbative ambiguities of the Landau gauge condition [90], evidence has been found that the IR behaviour especially of the ghost propagator might strongly depend on the choice of the Gribov copy on the residual gauge orbit [9]. This corresponds to the choice of boundary conditions in functional methods [6].

In the strong coupling limit [10, 11, 12, 91], simulations have likewise also been performed for $d < 4$ [13, 92]. The interpretation of the results is still under debate. It has been argued that the lattice data are compatible with a scaling branch for a subset of lattice momenta [10], but also that they definitely disprove such a behaviour [92]. Very recent additional results provide strong evidence for the severity of the Gribov problem, especially regarding the ghost propagator [13].

B. Gauge fixing problem on the lattice

Since the ghost and gluon propagator are gauge-dependent quantities, their calculation requires to sample configurations from the gauge fixing surface $\Gamma = \{A_\mu(x) | \partial_\mu A_\mu(x) = 0\}$. Fixing to lattice Landau gauge amounts to maximising a gauge fixing functional whose Hessian is the Faddeev-Popov operator $-\partial_\mu D_\mu^{ab}[A]$, where D_μ is the covariant derivative. Thus, after gauge fixing, all configurations are located inside the Gribov region $\Omega = \{A_\mu(x) | -\partial D[A] > 0\}$. However, Ω still contains gauge copies, in contrast to the fundamental modular region $\Lambda \subset \Omega$. On the lattice, reaching Λ is equivalent to obtaining the *global* maximum of the gauge fixing functional

$$R = \frac{1}{N_c V d} \sum_{x,\mu} \text{Re tr } U_\mu(x). \quad (7)$$

This poses an NP-hard optimisation problem, equivalent to finding the ground state of a spin glass [93, 94].

III. STOCHASTIC QUANTISATION ON THE LATTICE

A. Stochastic gauge fixing

As already discussed in the introduction, there is quite some evidence that Landau gauge fixing on the lattice still severely suffers from the Gribov problem. This already motivates the choice of an alternative lattice gauge fixing algorithm.

Stochastic quantisation is a method introduced in a more general context in [14]. Within stochastic quantisation gauge fixing can be implemented via a gauge fixing force [20]. An infinitesimal gauge transformation in the Langevin equation for the gauge field is given by

$$\frac{\partial A_\mu^a}{\partial t} = -\frac{\delta S_{\text{YM}}}{\delta A_\mu^a} + D_\mu^{ab} v^b + \eta_\mu^a. \quad (8)$$

Here, $v^b = \alpha^{-1} \partial_\mu A_\mu^b$ with a gauge fixing parameter α , and η_μ^a is Gaussian white noise with the properties

$$\begin{aligned} \langle \eta_\mu^a(x, t) \rangle &= 0, \\ \langle \eta_\mu^a(x, t) \eta_\nu^b(x', t') \rangle &= 2\delta_{ab} \delta_{\mu\nu} \delta(t - t') \delta(x - x'). \end{aligned} \quad (9)$$

Due to Zwanziger's gauge fixing term, the equilibrium configurations of this equation are fixed to Landau gauge. It can be shown [25] and has been demonstrated numerically [21] that this equilibrium is stable only inside Ω .

While stochastic gauge fixing cannot be expected to restore global BRST invariance, it is a priori possible that it might sample the configuration space differently from standard gauge fixing. E.g., it might give us a *uniform* gauge fixing on the first Gribov region Ω . Note in this context that the statistical arguments in favour of the Gribov-Zwanziger scenario only work if the gauge fixing does not single out some region inside the first Gribov region in the thermodynamical limit. A uniform distribution avoids such a possibility.

On the other hand, stochastic quantisation is unlikely to provide us with a tool for a unique gauge fixing in the fundamental modular region Λ , since it does not even aim at the global maximisation of the gauge fixing functional R . But this fact might not harm its prospects for two reasons: First, even sophisticated algorithms designed to better approximate the global maximum of the functional R do not yield the scaling solution on the lattice [82, 83, 95, 96, 97]. Second, the FMR and the Gribov region should be equivalent in the thermodynamical limit according to a conjecture by Zwanziger [3]. So, if stochastic quantisation leads to a uniformly covered Gribov region, this might be already sufficient.

B. Lattice formulation

We simulate quenched $SU(2)$ with the group elements conveniently parametrised as

$$U_\mu(x) = u_\mu^0(x) + i\sigma^a u_\mu^a(x). \quad (10)$$

Unquenching effects are discussed in [79], and $SU(3)$ is treated in [81, 86, 98, 99]. A comparison of $SU(3)$ and $SU(2)$ is specifically interesting as most continuum implementations with functional methods use approximations which are insensitive to $1/N_c$ -effects.

The lattice formulation of the Langevin equation, initially without Zwanziger's drift term, is [15]

$$U_\mu(x) \rightarrow \exp(i\sigma^a R_{\mu x}^a) U_\mu(x), \quad (11)$$

with R composed of the Lie derivative of the standard Wilson plaquette action [100], providing the dynamical drift force F , and a stochastic term,

$$R_{\mu x}^a = \varepsilon F_{\mu x}^a + \sqrt{\varepsilon} \eta_{\mu x}^a \quad (12)$$

$$F_{\mu x}^a = i\nabla_{\mu x}^a S[U]. \quad (13)$$

In addition, we have implemented a random walk method, whose results agree with those obtained from Langevin evolution. In this case, the form of an individual update is

$$U_\mu(x) \rightarrow \exp(i\sigma^a A_\mu^a(x)) U_\mu(x), \quad (14)$$

and $A_\mu^a(x)$ is determined, starting from zero, by accepting updates

$$A_\mu^a(x) \rightarrow A_\mu^a(x) \pm \eta \quad (15)$$

with probability

$$p = \frac{1}{2} \left(1 \pm \tanh \left(\frac{1}{2} \eta F_{\mu x}^a \right) \right). \quad (16)$$

Regardless of the method used for the dynamic updates, Zwanziger's additional drift force is implemented as a lattice gauge transformation, sc. $U_\mu(x) \rightarrow \Omega(x)U_\mu(x)\Omega^\dagger(x + \hat{\mu})$ with [23, 24, 25]

$$\Omega(x) = \exp \left(-i \frac{\beta}{2N_c} \Delta^a \sigma^a \frac{\varepsilon}{\alpha} \right). \quad (17)$$

Here, Δ^a is the lattice version of the Landau gauge condition,

$$\Delta^a(x) = \sum_{\mu=0}^{d-1} (u_\mu^a(x) - u_\mu^a(x - \hat{\mu})). \quad (18)$$

By means of this implementation, the gauge force moves are not only tangential to a gauge orbit, but strictly on the orbit.

We interchange the updates (11) and the gauge transformations 'locally', i.e., such that a gauge transformation of all affected link variables is performed after each single link update. This serves to minimize the distance to the gauge fixing surface during the updates, measured by Δ^2 , the average of $\Delta^2(x)$. However, Δ^2 does not decrease monotonically when α is lowered (fig. 1), which presumably is due to an 'overshooting' effect.

For a high precision of gauge fixing, we usually amend an interchange of dynamical and gauge fixing steps as described above by standard stochastic overrelaxation (STOR) [101]. While this goes, strictly speaking, beyond the scheme of stochastic gauge fixing, it hardly affects the 'locality' of the latter. An alternative possibility would be to choose a step size small enough to render the 'amendment' dispensable, cp. the decrease of Δ^2 with the step size in fig. 1. But this would require so small a step size that the autocorrelation time would become unacceptably large for practical simulations.

In contrast, we refer by the term 'standard gauge fixing' to a usual heat-bath thermalisation [102] followed by STOR. This is a 'global' procedure, as the thermalisation takes place far away from Γ , i.e., at large Δ^2 . The difference is sketched in fig. 2.

C. Return cycles

It has early been demonstrated [21] that a start outside the Gribov horizon leads to 'return cycles' during which the distance from the gauge fixing surface temporarily increases, i.e., the system returns to the Gribov region by

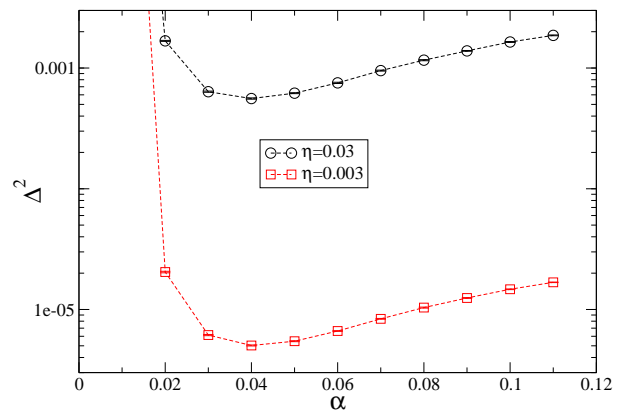


FIG. 1: Illustration of the change of Δ^2 with the gauge fixing parameter α on a 48^2 lattice for two different random walk step sizes.

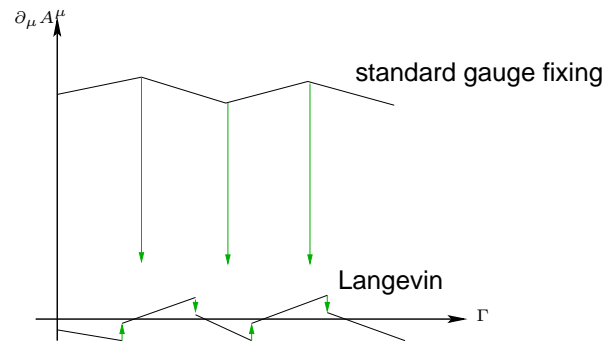


FIG. 2: Qualitative illustration of a difference between stochastic and standard gauge fixing. The green arrows denote gauge fixing steps, the black lines connecting them denote dynamic updates. A similar picture appeared already in [28].

a path outside the gauge fixing surface. This is expected since only gauge-fixed configurations inside the Gribov region are stable equilibrium configurations. This is by itself not a special property of the gauge force, as it is shared by every algorithm that performs numerical gauge fixing. But a priori, the return cycles might play a role in bringing about a certain distribution in configuration space, see subsec. VIB.

The existence of return cycles is readily confirmed by the numerics. By starting the system outside the Gribov region, e.g., at sufficiently large constant gauge field, and measuring the lowest nontrivial eigenvalue of the Faddeev-Popov operator during the stochastic evolution, we can indeed confirm that the configurations move towards the Gribov region, in accordance with an intuitive picture, see fig. 3. The lowest eigenvalue λ_0 increases monotonically, while the distance from the gauge fixing surface reaches a maximum before decreasing again, as indicated by the behaviour of Δ^2 .

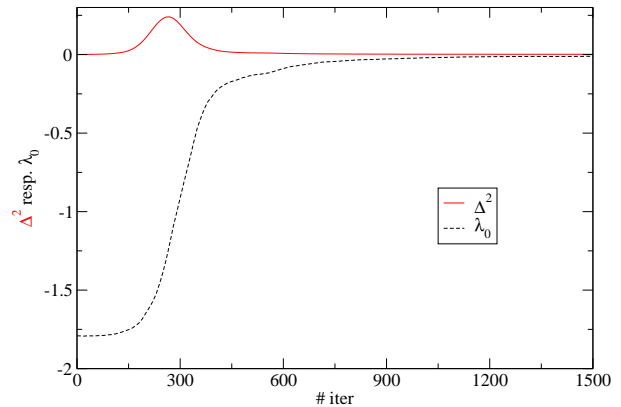
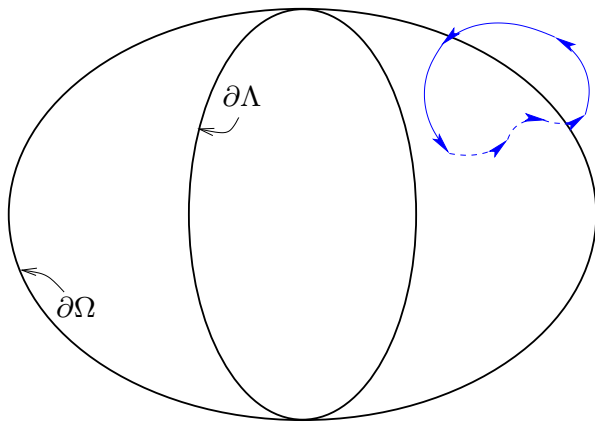


FIG. 3: *Left (a)*: Qualitative illustration of a return cycle. *Right (b)*: Numerical data. Approach to Ω during a return cycle with the Langevin algorithm (24²). Black: Lowest nontrivial FPO eigenvalue ($\hat{=}$ distance to $\partial\Omega$), red: distance to gauge fixing surface.

IV. STOCHASTIC QUANTISATION IN A TOY MODEL

Before we present the bulk of our results on stochastic gauge fixing in $SU(2)$ lattice gauge theory in sec. V, we find it useful to illustrate some issues related to stochastic gauge fixing and the configuration space in QCD by means of a simple toy model.

A. Motivation

The toy model we employ is a slightly modified generalisation of a two-dimensional model used to illustrate some properties of stochastic gauge fixing in [22]. Note that a different toy model for stochastic gauge fixing has been studied in [103]. As a modification of the model from [22], we have chosen the sign of the action such that the dynamical effects and the gauge fixing effects can be clearly distinguished. The generalisation consists in extending the model to a higher number of dimensions. It is motivated by the possibility of observing an ‘entropy effect’ that leads to an accumulation of configurations close to the ‘Gribov horizon’ of this model, since such configurations should account for confinement in QCD according to the Gribov-Zwanziger scenario. Hence the model could give an idea about the dependence on the three effects: the gauge fixing force, the dynamics of the action and the entropy.

B. The toy model

In the model, the variables $x_i \in \mathbb{R}$ ($i \in \{1, \dots, n\}$) and $y \in \mathbb{R}$ are subject to two forces, a gauge fixing force and a force derived from an action. The former reads

$$\begin{pmatrix} \dot{y} \\ \dot{x}_i \end{pmatrix} = \begin{pmatrix} K_0^g \\ K_i^g \end{pmatrix} = -\frac{1}{\alpha} \begin{pmatrix} (1-x^2)y \\ 2x_i y^2 \end{pmatrix}, \quad (19)$$

where $x^2 = \sum_{i=1}^n x_i^2$ and the gauge fixing parameter α is positive. Notice that this force is not the gradient of an action. It drives the configurations towards the gauge fixing surface $y = 0$. The set

$$\Omega = \left\{ \begin{pmatrix} y \\ \vec{x} \end{pmatrix} \middle| y = 0, x < 1 \right\} \quad (20)$$

may be referred to as the ‘Gribov region’ of this model. This terminology is sensible because the Gribov region is where all configurations are in the limit of perfect gauge fixing – and because the asymptotic distribution for $\alpha \rightarrow 0$ is

$$dP(x, y) \propto x^{n-1} (1-x^2) \theta(1-x^2) \delta(y) dx d\Omega dy, \quad (21)$$

where $d\Omega$ is understood as the differential solid angle in n dimensions.

The ‘Faddeev-Popov determinant’ of this model is $-\alpha^{-1}(1-x^2)$, which is proportional to (21) only for $n = 1$ and vanishes, like (21), linearly near the horizon $x = 1$. The FP operator is obtained from the linearisation $\frac{d}{dt}v = hv$, with $v = 0$ the gauge condition, thus here $v = y$.

The distribution (21) is maximal at $x = \sqrt{\frac{n-1}{n+1}}$. The maximum approaches the ‘Gribov horizon’ $\partial\Omega$ as n grows. It is interesting to see whether stochastic gauge fixing supports this effect. Obviously, the gauge fixing force is orthogonal to the gauge fixing surface in its immediate vicinity, see fig. 4, since this surface is the equilibrium of the gauge force. In addition, fig. 4 illustrates that this equilibrium is stable only for $x < 1$, which justifies the definition (20) of the ‘Gribov region’.

C. Numerical simulation

To see explicitly the effects of the various parameters, a numerical simulation of this toy model is easily possible, e.g. by means of a random walk algorithm, in which

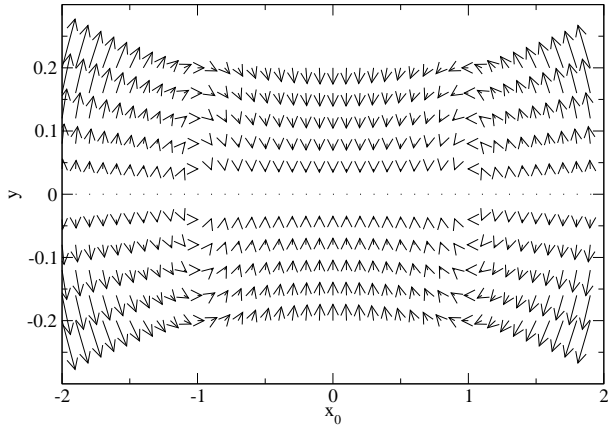


FIG. 4: The gauge fixing force of the toy model for $n = 1$, $\alpha^{-1} = 0.15$.

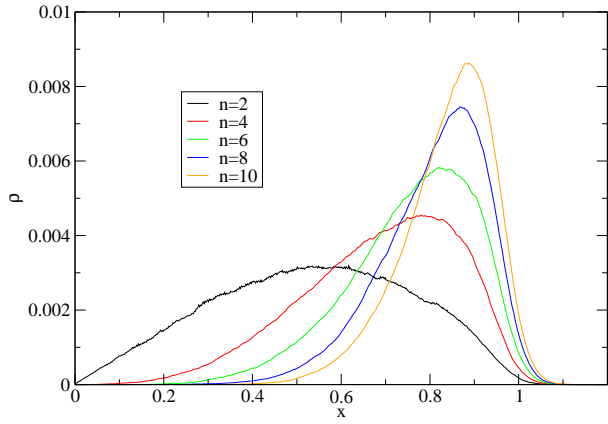


FIG. 5: ‘Entropy effect’ for the (not gauge-invariant) distribution of values of x at the parameters $\alpha = 5 \cdot 10^{-5}$, $\beta = 0$, step size $\eta = 0.001$.

the probability for a local update with fixed step size η (introducing $\{x_\nu\}$, $\nu = 0, \dots, n$ with $y \equiv x_0$) is given by

$$p(x_\nu \rightarrow x_\nu \pm \eta \hat{e}_\nu) = \frac{1}{2} \pm \frac{1}{2} \tanh\left(\frac{\eta}{2} K_\nu(\{x_\mu\})\right). \quad (22)$$

A gauge-invariant dynamics may be defined from the orbits

$$u_i = x_i \exp\left(-\frac{x^2}{2} - y^2\right) (= \text{const.}), \quad i = 1, \dots, n \quad (23)$$

as

$$S = \beta u^2, \quad u^2 = \sum_{i=1}^n u_i^2. \quad (24)$$

S is monotonously increasing for $0 \leq x \leq 1$ and has therefore the effect of driving the configurations toward $x = 0$, similarly to the expected effect of the QCD action.

The dynamical part of the force is given by

$$K_\nu^a = -\frac{dS}{du} \frac{du}{dx_\nu}, \quad (25)$$

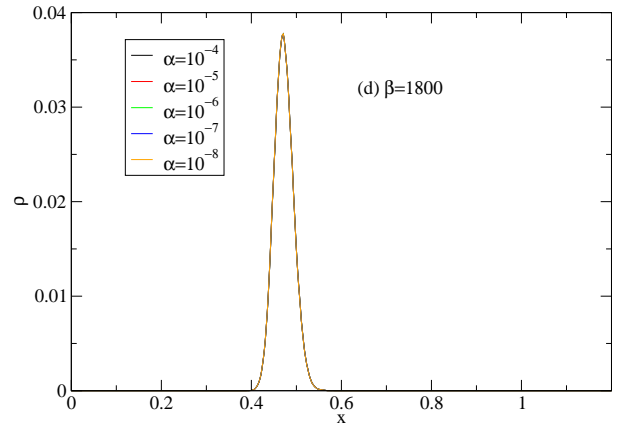
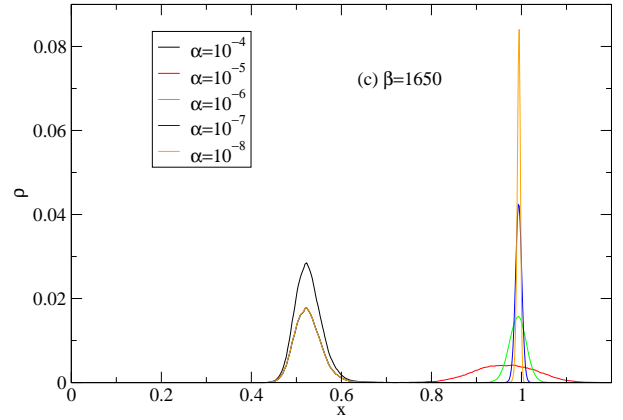
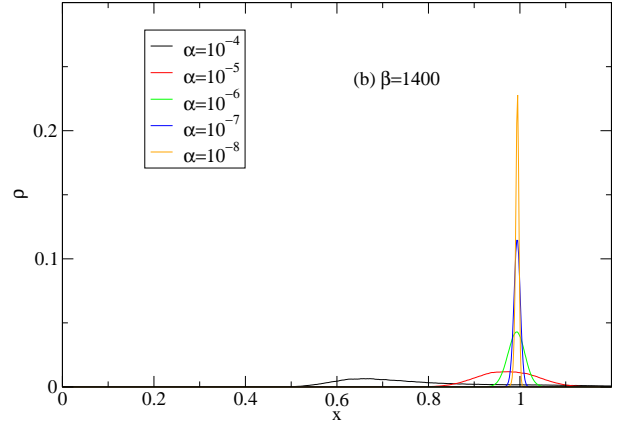
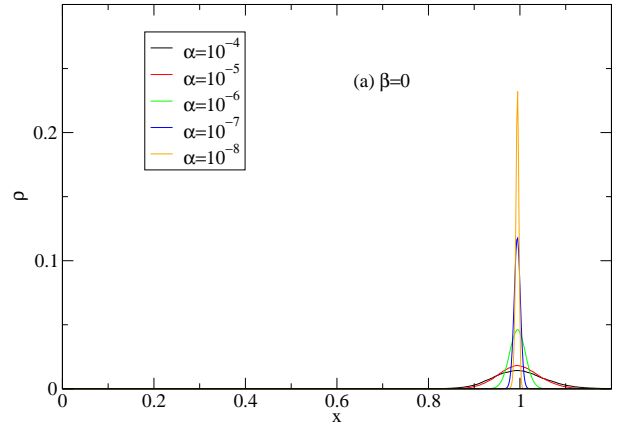


FIG. 6: Increasing β , the strength of the gauge action, at $n = 500$ for $\alpha = 10^{-4}, \dots, 10^{-8}$. Values of β indicated in the plots. Step size $\eta = 10^{-4}$.

and the drift force of the random walk algorithm, eq. (22), is

$$K_\nu = K_\nu^a + K_\nu^g. \quad (26)$$

In the following figures we show the distribution of gauge-fixed configurations, $\rho(x)$. The increasing proximity of the configurations to the Gribov horizon with larger n is illustrated in Fig. 5. The effect of the gauge fixing force is as expected, since the numerical results obey the distribution (21). The most interesting observations pertain the combined effect of the three parameters: n, α and β . As illustrated in Fig. 6, keeping n fixed, the action has little effect up to some value of β (compare figs. 6a and 6b), and then suddenly starts driving the configurations toward the interior of the Gribov zone, selectively depending on α , see figs. 6c and 6d. This happens at smaller values of β for lower n .

Notice that in all cases there is a small proportion of configurations just outside the Gribov horizon. This is due to the fact that the confinement to the Gribov region is achieved by return cycles engendered by the unstable modes which K^g develops beyond the horizon, see fig. 4. The fraction of configurations outside the Gribov horizon shrinks as the strength of the gauge fixing force increases, see fig. 6a.

The lesson from this toy model is then that there are subtle and non-linear effects in the combined action of the gauge fixing, the gauge dynamics and the entropy, and we should not be amazed to find such non-trivial behaviour in the realistic case of lattice gauge theory.

V. RESULTS FOR THE GLUON AND GHOST PROPAGATOR

A. Technicalities

The relation between the continuum and the lattice momenta is, as usual,

$$q_\mu(k_\mu) = \frac{2}{a(\beta)} \sin\left(\frac{\pi k_\mu}{L_\mu}\right). \quad (27)$$

We impose the cylinder cut [104] on the momenta. The propagators have been renormalised at $\mu = 2.5$ GeV. For some details concerning the implementation of the ghost propagator, see subsec. V C.

We compare our results for the IR exponents with the ‘scaling predictions’ [31], which are $\kappa = 0.2$ in $d = 2$, $\kappa \approx 0.4$ in $d = 3$ and $\kappa \approx 0.6$ in $d = 4$, with κ_A determined by eq. (6), see II.

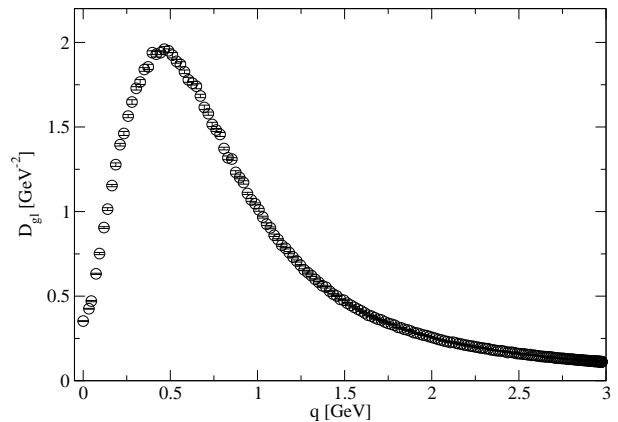


FIG. 7: Gluon propagator on a 200^2 lattice at $\beta = 10$ ($a = 0.082$ fm).

B. Gluon propagator

We have calculated the scalar gluon propagator function in two, three and four dimensions,

$$D_{\text{gl}}(k) = \frac{1}{N_c^2 - 1} \frac{1}{d - 1} \sum_{\mu, a} \langle A_\mu^a(k) A_\mu^a(-k) \rangle, \quad (28)$$

with the standard lattice discretisation of the gauge field, $A_\mu^a(x) \propto u_\mu^a(x)$. We find significant differences between stochastic and standard gauge fixing at relatively large Δ^2 . In turn, if we fix the gauge to a high precision, $\Delta^2 \leq 10^{-15}$, the differences disappear, and we confirm previous lattice results in all dimensions. Notice that at large Δ^2 the picture is complicated by the fact that the results of standard STOR after a heat-bath thermalisation strongly depend on the value of p , which fixes the probability of non-optimal gauge transformations in the STOR algorithm. The differences mentioned are directly related to the distance from $\partial\Omega$, which is visible from the spectrum of the Faddeev-Popov operator, see section VI.

1. Two dimensions

The two-dimensional case is special; there are analytical results for, e.g., the string tension [105], and the existence of scaling behaviour has been viewed as relatively uncontroversial also from lattice data [75, 76]. Our results for this case appear to corroborate the latter findings. The data are shown in fig. 7. We extract the infrared exponent $\kappa_A = -1.37$, which corresponds to $\kappa = 0.19$ if eq. (6) is assumed to hold. This extraction is done via a power law fit to the five most IR data points after discarding the two lowest non-vanishing momenta, which closely resembles the method employed in [75]. χ^2/ndf is safely below 1. As the value of κ nicely agrees with the prediction of 0.2, this appears to speak in favour of the scaling solution in 2D on the lattice, corroborating previous results obtained with standard gauge

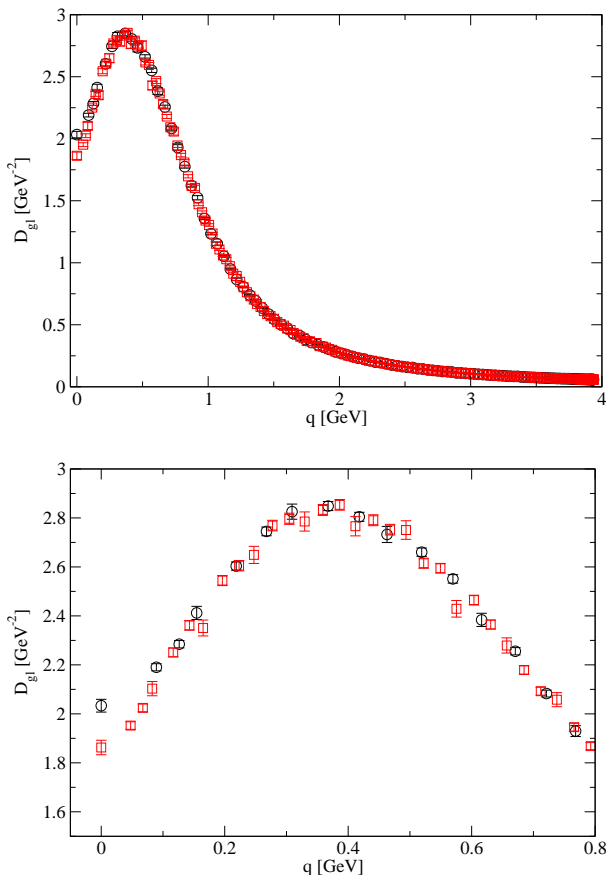


FIG. 8: *Top (a)*: Gluon propagator in 3D at $\beta = 4.2$ ($a = 0.17$ fm) on 80^3 (black circles) and 150^3 (red squares). *Bottom (b)*: Blowup of the same data in the IR.

fixing [75, 76]. Even more importantly, a comparison with the ghost propagator (subsec. VC) shows that the scaling relation (6) is approximately fulfilled. Note, however, the surprising fact that the naive scaling hypothesis even fails in two dimensions at $\beta = 0$, see [13]. Here it has been found that while approximate scaling holds true for the gluon propagator for intermediate momenta, the ghost propagator is subject to drastic changes if changing the global properties of the gauge fixing.

2. Three dimensions

In three dimensions, it has been observed in lattice simulations [89] that the gluon propagator peaks at $q = 350_{-50}^{+100}$ MeV, but still approaches a non-vanishing value in the infrared, $D(q^2 \rightarrow 0) > 0$. We confirm this observation with stochastic gauge fixing on a 150^3 lattice at $\beta = 4.2$ ($\approx (26 \text{ fm})^2$), see fig. 8. Furthermore, we observe a sign of a finite volume effect when comparing the data to the 80^3 case (blowup in fig. 8b). In agreement with previous results for $d = 3$ [80], there is no evidence that this suffices to yield the scaling solution as the volume $V \rightarrow \infty$.

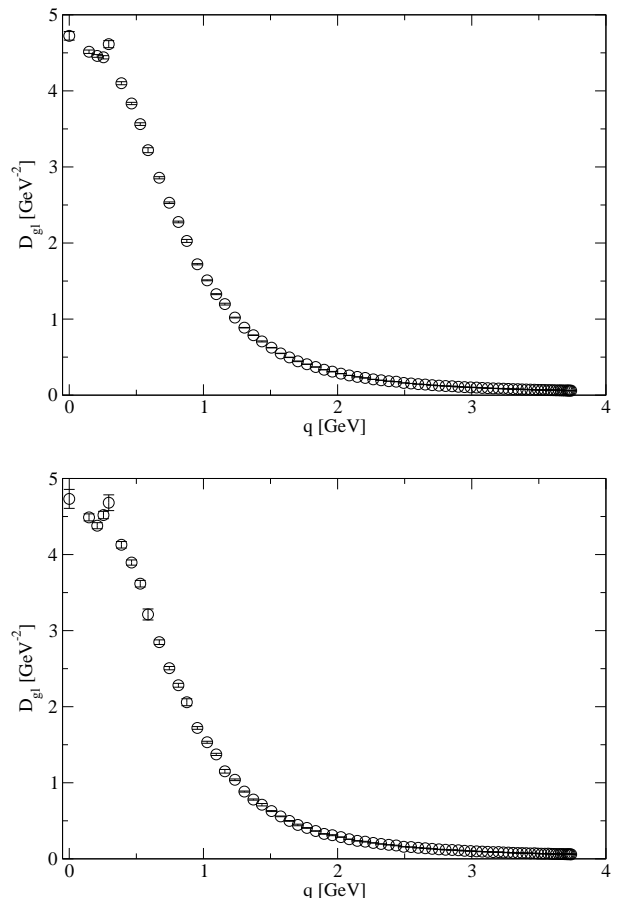


FIG. 9: *Top (a)*: Gluon propagator, 40^4 , $\beta = 2.2$ ($a = 0.21$ fm). *Bottom (b)*: For comparison, the result of a simulation with lower g.f. accuracy, sc. only $\Delta^2 < 10^{-8}$, but where also the ‘fine-tuning’ is done by stochastic gauge fixing (see text).

This is compatible with the findings in [13] for $\beta = 0$. There it has been shown that the scaling window within a standard gauge fixing moves towards larger momenta. Naively translated to non-vanishing β , this suggests that the assumed scaling region has to be washed out by the dynamics if we go to higher dimensions.

For comparison, we have also performed simulations with standard gauge fixing on a 150^3 lattice, which yield a gluon propagator essentially identical with the one obtained from stochastic quantisation.

3. Four dimensions

For $d = 4$, we again confirm earlier lattice results [80, 81] for sufficiently accurate stochastic gauge fixing. The gluon propagator on a 40^4 lattice at $\beta = 2.2$ is, like in 3D, clearly finite in the IR. Unlike in 3D, it does not possess a peak at finite momentum, see fig. 9. $V \approx (8.4 \text{ fm})^4$ is below the maximal lattice size already investigated with standard methods e.g. in [80, 99]. But the lower-

dimensional results, including those on the spectrum of $-\partial D$, sec. VI, suggest that the problem is not a finite volume effect, but may rather be the well-known gauge fixing problem, as laid out in sections I and II.

Our value of the gauge functional $R = 0.8278(1)$ essentially agrees with the value obtained from standard gauge fixing, while it is significantly below the value after improved gauge fixing aimed specifically at maximising R [95]. Here, ‘standard gauge fixing’ denotes a method of choosing first copies after overrelaxation, and ‘improved g.f.’ refers to employing simulated annealing and \mathbb{Z}_2 flips. This is consistent with our other findings, indicating that the effect of stochastic gauge fixing is similar to the one of standard g.f., which renders the putative lattice gauge fixing problem more general.

Since our fine-tuning by stochastic overrelaxation may change the location of the sampled Gribov copies, we have also produced some results where the fine-tuning has been performed entirely within the scheme of stochastic quantisation. In case of a random walk implementation, this amounts to decreasing $\eta \rightarrow 0$ by some prescription, e.g., exponentially. Even though the accuracy of gauge fixing has been lessened here, the result is virtually the same, see fig. 9b.

C. Ghost propagator

The ghost propagator on the lattice is given by

$$D_{\text{gh}}(k) = \sum_{x,y} \left\langle (\mathbf{M}^{-1})_{xy}^{ab} \right\rangle e^{ik \cdot (x-y)}, \quad (29)$$

with $k \cdot x = 2\pi \sum_{\mu} k_{\mu} x_{\mu} / L_{\mu}$. Its calculation is computationally expensive, since it requires the inversion of the lattice Faddeev-Popov operator \mathbf{M} , whose standard form may be found e.g. in [12]. We have implemented both the point source method, see e.g. [106], and the plane wave source method, see e.g. [107]. This means that \mathbf{M} is inverted either on a point source $s_b^{a,x} = \delta^{ab}(\delta_{x,0} - 1/V)$ or a vector of plane waves $s_b^{a,x}(k) = \delta^{ab} e^{ik \cdot x}$. While the former method leads to heavy fluctuations in the UV, the latter one is much more time-consuming. The results shown here have been produced with a plane wave source, but sometimes inverting the Faddeev-Popov operator only on a proper subset of the momenta surviving the cylinder cut.

In two dimensions ($d = 2$), we extract from the ghost propagator, like from the gluon propagator, an infrared exponent close to the expected value $\kappa = 0.2$, sc. $\kappa = 0.17$. The basic fitting method is the same as for the gluon data, see VB 1. See fig. 10a for results on a rather large lattice.

For $d = 3$, we expect to see a finite-volume effect for the ghost propagator for the volumes used here, 40^3 and 80^3 . A fit of the 40^3 data in fig. 10 to a power law yields $\kappa = 0.25$, which is already clearly below ≈ 0.4 , i.e., the ‘scaling prediction’. A fit of the 80^3 data in fig. 10 to a

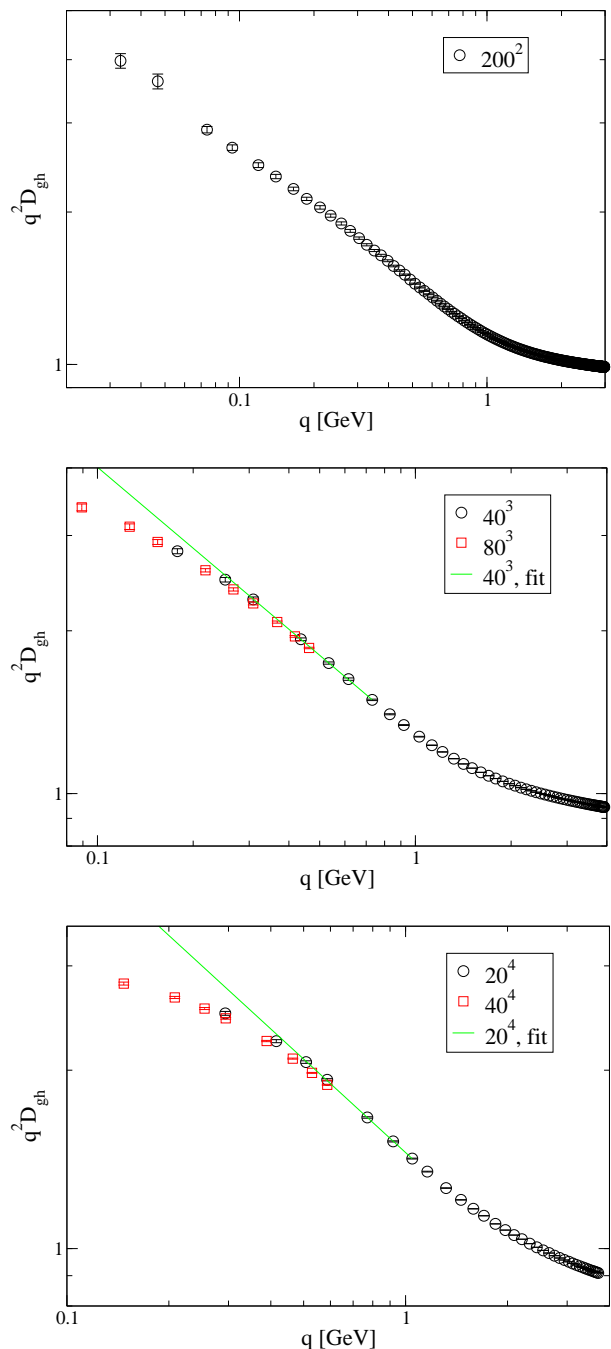


FIG. 10: Ghost dressing function in (a) $d = 2$ (top), (b) $d = 3$ (middle) and (c) $d = 4$ (bottom), at $\beta = 2.2, 4.2$ and 10, respectively.

power law yields $\kappa \approx 0.2$, indicating clear finite volume effects.

For $d = 4$, a similar effect is apparent from fig. 10c. On a small lattice, sc. 20^4 , we obtain $\kappa = 0.26$. Again, this is far below the ‘scaling prediction’ of ≈ 0.6 . The discrepancy is significantly larger than for $d = 3$. Moreover, the scaling relation (5) is violated thereby, given the gluon result of $\kappa_A = -1$ (subsubsec. VB 3), which

implies $\kappa = 0.5$ under (5). On the larger lattice, the IR behaviour is again harder to fit precisely, but clearly less divergent. Here, we have produced additional data with the point source method. This introduces heavy fluctuations in the UV, but does less harm in the IR, which is our focus of interest here. From these data, we obtain $\kappa = 0.19$. – The fact that κ doesn't vanish may well be due to the finite lattice extension [83, 108] or also to choosing the first instead of the ‘best’ Gribov copy [97].

VI. SPECTRUM OF THE FADDEEV-POPOV OPERATOR

A. Motivation and technicalities

As the first Gribov region Ω is the set of configurations with positive Faddeev-Popov operator (FPO), $-\partial D > 0$, the lowest eigenvalue of $-\partial D$ vanishes at the Gribov horizon $\partial\Omega$. Hence, its value may be interpreted as a measure of the distance from $\partial\Omega$. This is an interesting test of the Gribov-Zwanziger scenario of confinement, since this predicts that configurations near $\partial\Omega$ account for confinement. The lattice discretisation of the FPO is a $3V \times 3V$ real symmetric matrix. Previous lattice studies have established that the gauge copies tend to move towards the Gribov horizon as V is increased, and away from it as the gauge fixing is improved, i.e., as R is increased [109, 110].

We want to compare the spectra after stochastic and standard gauge fixing. The fact that we intend to do so also at insufficient gauge fixing (i.e., relatively large Δ^2) imposes a restriction on the method used to extract the eigenvalues of the FPO. In particular, we cannot assume that the Faddeev-Popov matrix is positive definite. This prevents us from applying the conjugate gradient method for the matrix inversion and exploiting its connection to the Lanczos algorithm for finding a subset of its eigenvalues [111]. Thus, we find *all* eigenvalues of the $3V \times 3V$ Faddeev-Popov matrix with a standard algorithm for real symmetric matrices, sc. symmetric bidiagonalisation and QR reduction, which is rather impracticable on large lattices.

The standard lattice discretisation of the FPO which we use is the Hessian of the gauge fixing functional (7). As usual, terms that vanish under the gauge fixing condition are omitted. To employ this discretisation also at imperfect gauge fixing is clearly not a unique choice, but has the advantage that the three zero modes of the FPO exist to a better approximation. The ‘lowest nontrivial FPO eigenvalue λ_0 ’ is always understood without these three trivial eigenvalues. While this choice requires inferences from the value of λ_0 to the distance to the Gribov horizon to be taken with a grain of salt, it still permits a qualitative comparison between stochastic and standard gauge fixing.

B. Results

A few results on the Faddeev-Popov eigenvalues have already been presented in the analysis of return cycles, subsec. III C; the bulk of results is shown in the following.

While we have investigated the full Faddeev-Popov operator spectrum mainly on tiny lattices, like 24^2 , the picture we have obtained is rather unambiguous. Let us first state the results for stochastic gauge fixing, i.e., random walk steps with ‘locally’ included gauge fixing. At some intermediate Δ^2 , i.e., at a not very small distance from Γ , the distribution of the lowest non-vanishing eigenvalue of the Faddeev-Popov operator after stochastic gauge fixing shows a very pronounced peak close to the Gribov horizon. The peak is located slightly outside the Gribov horizon, see fig. 11 (upper plots). This implies that Landau gauge is not fixed properly at this Δ^2 , since $-\partial D$ is the Hessian of $\int d^4x |gA|^2$, which is minimised by numerical Landau gauge fixing.

In the case of standard gauge fixing, i.e., STOR gauge fixing after heat-bath thermalisation, the distribution of λ_0 exhibits a twofold dependence on Δ^2 and the STOR parameter p . It resembles its counterpart from stochastic gauge fixing only around some specific value of p . Let us spell this out in more detail. At intermediate Δ^2 and large p , the procedure yields a peak at some distance from the horizon and clearly inside of it. When the accuracy of the standard gauge fixing is further lowered by stopping STOR at a larger Δ^2 , the distribution is shifted outside of the horizon, without a peak especially close to $\partial\Omega$. At intermediate Δ^2 , we compare different values of p . At small p , much more configurations are outside the horizon, and at intermediate p , the observation from stochastic gauge fixing is qualitatively reproduced, see fig. 11 (lower plots). Interestingly, the latter value roughly minimises the number of gauge fixing sweeps to obtain the desired value of Δ^2 . For sufficiently small Δ^2 , the distribution obtained from stochastic gauge fixing coincides with the one from standard gauge fixing regardless of p , and no bias towards the Gribov horizon remains. This is evident from the contrast between the left plots of fig. 11 and their counterparts at smaller Δ^2 , fig. 14.

Moreover, fig. 12 illustrates that at the same intermediate value of Δ^2 , the gluon propagator is less similar to the fully gauge-fixed result if more configurations are outside the Gribov region ($\lambda_0 < 0$). This difference is created, as described, by varying p . The gluon propagator at vanishing momentum is significantly anticorrelated with λ_0 , see fig. 13.

A peak close to $\partial\Omega$, but of course inside Ω is of interest especially for the Gribov-Zwanziger scenario of confinement, since it would imply that those configurations are preferably sampled which account for confinement according to this scenario. However, generating configurations at smaller Δ^2 by adjusting α and the step size does not help to generate such a peak: For small Δ^2 , the distributions from stochastic and standard gauge fixing

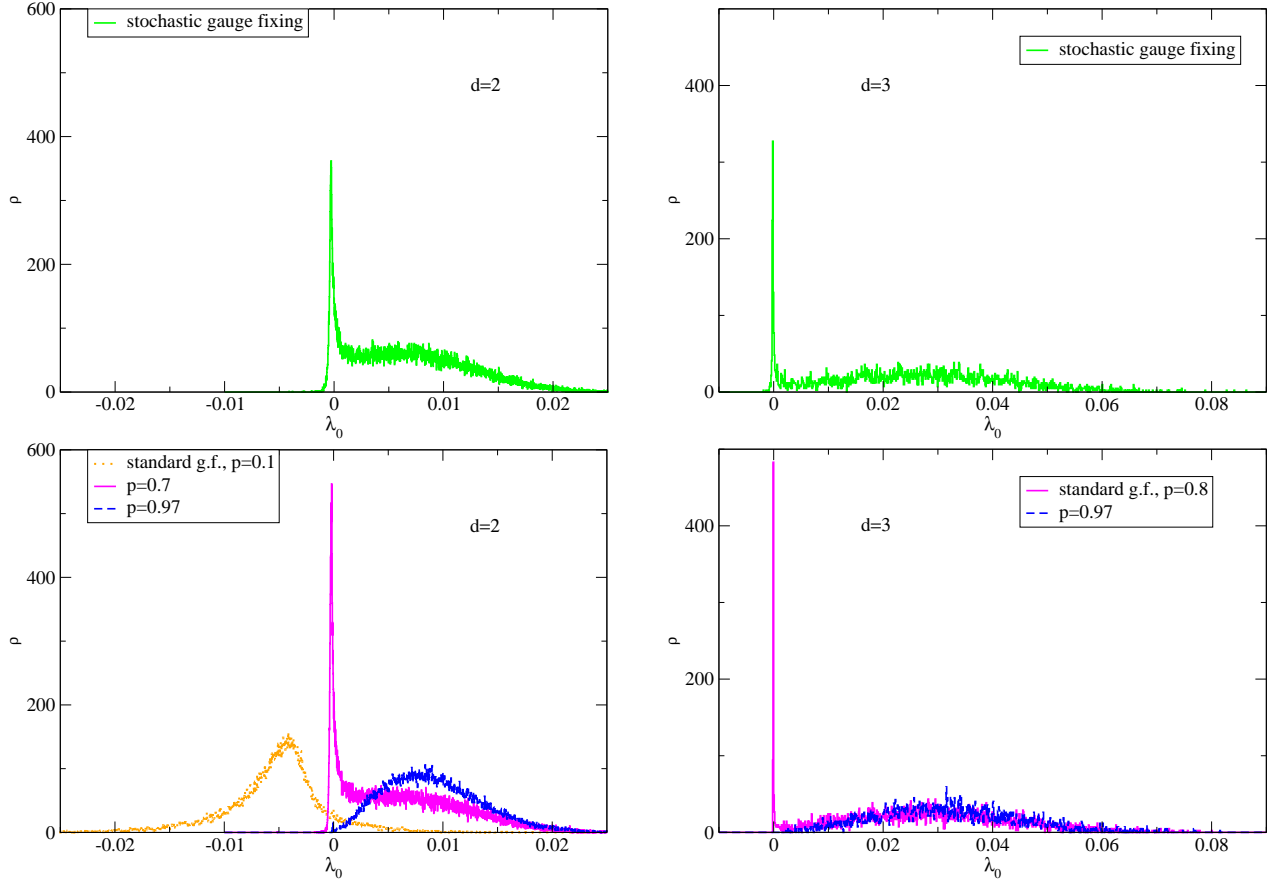


FIG. 11: Histograms of the lowest nontrivial FPO eigenvalue λ_0 in $d = 2$ resp. $d = 3$ from stochastic (*top*) and standard gauge fixing (*bottom*). *Left*: 24^2 , $\beta = 10$, $\Delta^2 \approx 8 \cdot 10^{-4}$. *Right*: 12^3 , $\beta = 4.2$, $\Delta^2 \approx 7 \cdot 10^{-4}$.

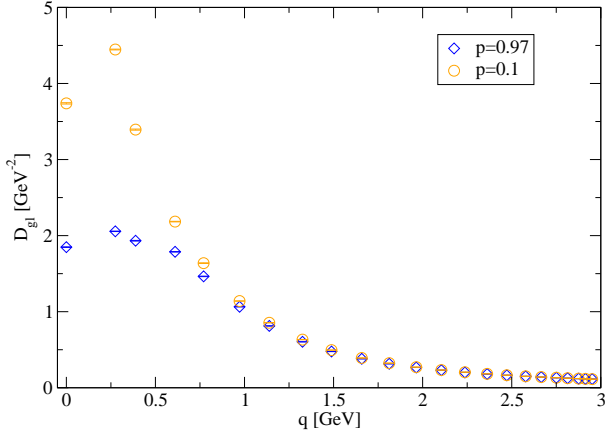


FIG. 12: Gluon propagators corresponding to the lower left plot of fig. 11.

become indistinguishable, regardless of p . This is also true if Δ^2 is lowered gradually by decreasing α and ε resp. η simultaneously.

It is possible to relate the distribution after stochastic gauge fixing at intermediate Δ^2 to a speculative scenario involving ‘return cycles’, see subsec. III C. In this in-

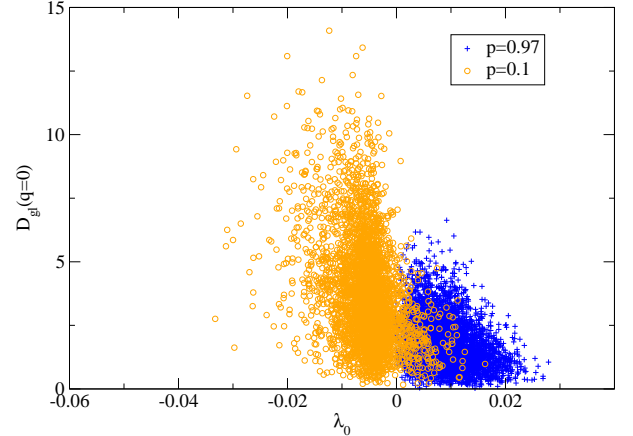


FIG. 13: Scatter plot of lowest FPO eigenvalue vs. gluon propagator at $q = 0$ for intermediate Δ^2 (data like in lower left plot of fig. 11). Correlation coefficient: $\rho = -0.40$ ($p = 0.1$, $N = 36000$ configurations) resp. $\rho = -0.29$ ($p = 0.97$, $N = 48000$). For clarity, only 10% of data points are shown.

tuitive picture, the Langevin evolution leads to an accumulation of the gauge-fixed configurations at the Gribov horizon.

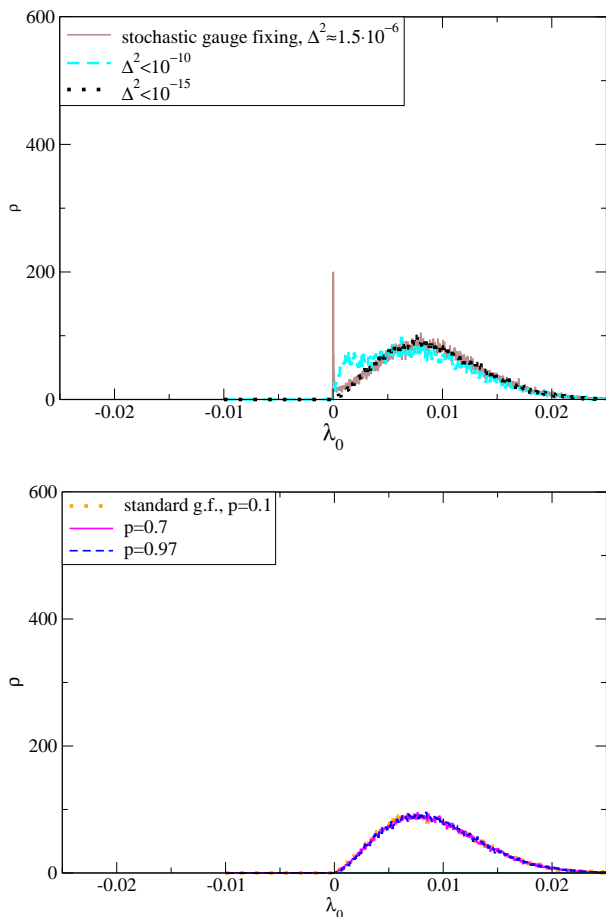


FIG. 14: Histograms of λ_0 on a 24^2 lattice at $\beta = 10$. *Top (a)*: Stochastic gauge fixing with increasing accuracy by choosing a small step size during the entire stochastic process ($\Delta^2 \approx 1.5 \cdot 10^{-6}$) resp. decreasing the step size for fine-tuning ($\Delta^2 < 10^{-10}$ and $\Delta^2 < 10^{-15}$). *Bottom (b)*: Standard gauge fixing with $\Delta^2 < 10^{-10}$ for different values of p .

Moreover, we find a strong anticorrelation between the IR ghost propagator and the lowest FPO eigenvalue, confirming findings of [109, 110] with standard gauge fixing; see fig. 15 (unrenormalised data). Note that on the larger lattices, we have not calculated all FPO eigenvalues, but rather employed the method of [111]. Thus, in fig. 15, ‘ λ_0 ’ does not refer to the strictly lowest eigenvalue, but to the smallest one as found by the Lanczos procedure related to the conjugate gradient method.

Finally, we also observe a finite volume effect, sc. that the lowest eigenvalue tends to be smaller on larger lattices, again like already reported in [109, 110].

VII. CONCLUSION

In the present work we have studied lattice Yang-Mills theory in Landau gauge within stochastic quantisation in two, three and four dimensions. We also have studied a finite-dimensional toy model in order to illustrate

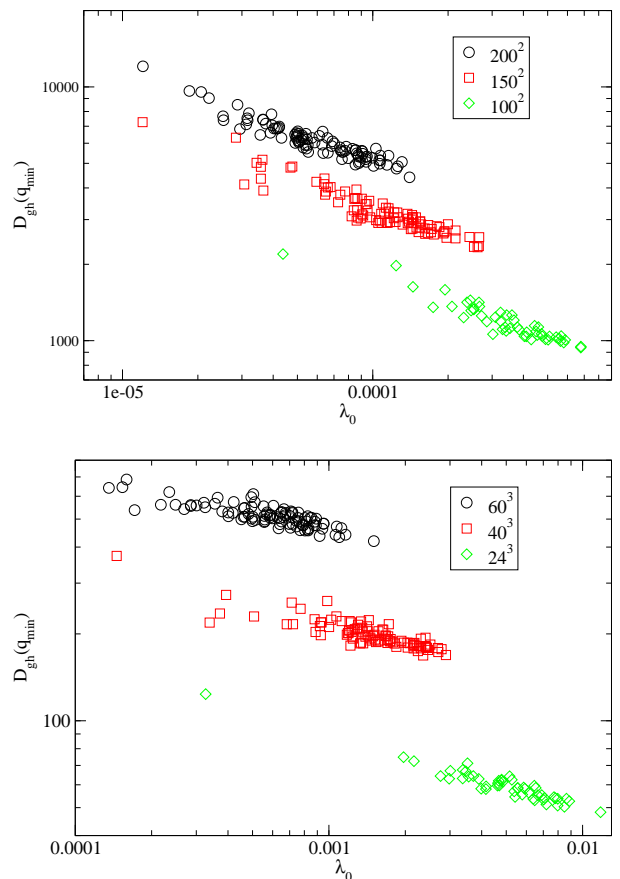


FIG. 15: Scatter plot of ghost propagator at lowest non-vanishing momentum vs. approximate lowest nontrivial FPO eigenvalue. *Top (a)*: $d = 2$. Correlation coefficient $r = -0.82$ resp. -0.83 in all three cases. *Bottom (b)*: $d = 3$. $r = -0.74$ resp. -0.79 in all three cases. Between 50 and 100 configurations per lattice size.

some subtleties of gauge-fixed Langevin evolutions. In this model we see an interplay between the dimensionality of the system, the gauge force and the dynamics induced by the action.

Our results for the ghost and gluon propagator and the low-lying eigenvalues of the Faddeev-Popov operator agree with the lattice results obtained so far with standard gauge fixing procedures. The detailed analysis revealed an interesting approach towards the final distribution on the first Gribov region if the gauge fixing is bettered. For worse gauge fixing quality the distribution shows also a sharp peak slightly outside the Gribov horizon. This implies a statistical bias towards the Gribov-Zwanziger scenario. We conclude that stochastic quantisation provides a tool of how to avoid a possible mechanism against the Gribov-Zwanziger scenario. Still this does not suffice to adjust the gauge fixing appropriately, i.e., to obtain on the lattice the full one-parameter family of solutions found in continuum studies. This could suggest that the gauge fixing problem on the lattice might be even more general than previously assumed.

Together with further evidence from $\beta = 0$ computation on the lattice [13], as well as recent work on Landau gauge fixings [9], our results hint at the severity of the Gribov problem in lattice simulations. We hope that this problem can be resolved in near future along the ways outlined in [9, 13], and in particular in [69, 112].

Acknowledgments

We thank M. Ilgenfritz, A. Maas, A. Nakamura, L. von Smekal and D. Zwanziger for discussions. This work is

supported by Helmholtz Alliance HA216/EMMI. D.S. acknowledges support by the Landesgraduiertenförderung Baden-Württemberg via the Research Training Group “Simulational Methods in Physics”. I.-O.S. is indebted to the MPI for Physics, München for hospitality. The numerical simulations were carried out on the compute cluster of the ITP, University of Heidelberg, and on bw-GRiD (<http://www.bw-grid.de>), member of the German D-Grid initiative.

-
- [1] V. N. Gribov, Nucl. Phys. **B139**, 1 (1978).
 [2] D. Zwanziger, Nucl. Phys. Proc. Suppl. **34**, 198 (1994).
 [3] D. Zwanziger, Phys. Rev. **D69**, 016002 (2004), hep-ph/0303028.
 [4] T. Kugo and I. Ojima, Prog. Theor. Phys. Suppl. **66**, 1 (1979).
 [5] J. Braun, H. Gies, and J. M. Pawłowski, PoS **CONFINEMENT8**, 044 (2008), 0708.2413.
 [6] C. S. Fischer, A. Maas, and J. M. Pawłowski, Annals Phys. **324**, 2408 (2009), 0810.1987.
 [7] L. von Smekal (2008), 0812.0654.
 [8] I. M. Singer, Commun. Math. Phys. **60**, 7 (1978).
 [9] A. Maas (2009), 0907.5185.
 [10] A. Sternbeck and L. von Smekal (2008), 0811.4300.
 [11] A. Sternbeck and L. von Smekal, PoS **CONFINEMENT8**, 049 (2008), 0812.3268.
 [12] A. Sternbeck and L. von Smekal, PoS **LATTICE2008**, 267 (2008), 0810.3765.
 [13] A. Maas, J. M. Pawłowski, D. Spielmann, A. Sternbeck, and L. von Smekal, work in preparation.
 [14] G. Parisi and Y.-s. Wu, Sci. Sin. **24**, 483 (1981).
 [15] G. G. Batrouni et al., Phys. Rev. **D32**, 2736 (1985).
 [16] P. H. Damgaard and H. Huffel, Phys. Rept. **152**, 227 (1987).
 [17] G. Aarts and I.-O. Stamatescu, JHEP **09**, 018 (2008), 0807.1597.
 [18] G. Aarts, Phys. Rev. Lett. **102**, 131601 (2009), 0810.2089.
 [19] J. Berges and I. O. Stamatescu, Phys. Rev. Lett. **95**, 202003 (2005), hep-lat/0508030.
 [20] D. Zwanziger, Nucl. Phys. **B192**, 259 (1981).
 [21] E. Seiler, I. O. Stamatescu, and D. Zwanziger, Nucl. Phys. **B239**, 201 (1984).
 [22] E. Seiler (1984), lectures given at the 23rd Internationale Universitätswochen für Kernphysik, Schladming, Austria, Feb 20-Mar 1, 1984.
 [23] P. Rossi, C. T. H. Davies, and G. P. Lepage, Nucl. Phys. **B297**, 287 (1988).
 [24] A. Nakamura and M. Mizutani, Vistas Astron. **37**, 305 (1993).
 [25] M. Mizutani and A. Nakamura, Nucl. Phys. Proc. Suppl. **34**, 253 (1994).
 [26] H. Aiso et al., Nucl. Phys. Proc. Suppl. **53**, 570 (1997).
 [27] A. Nakamura, I. Pushkina, T. Saito, and S. Sakai, Phys. Lett. **B549**, 133 (2002), hep-lat/0208075.
 [28] A. Nakamura, T. Saito, and S. Sakai, Phys. Rev. **D69**, 014506 (2004), hep-lat/0311024.
 [29] L. von Smekal, R. Alkofer, and A. Hauck, Phys. Rev. Lett. **79**, 3591 (1997), hep-ph/9705242.
 [30] L. von Smekal, A. Hauck, and R. Alkofer, Ann. Phys. **267**, 1 (1998), hep-ph/9707327.
 [31] C. Lerche and L. von Smekal, Phys. Rev. **D65**, 125006 (2002), hep-ph/0202194.
 [32] R. Alkofer, C. S. Fischer, and F. J. Llanes-Estrada, Phys. Lett. **B611**, 279 (2005), hep-th/0412330.
 [33] D. Zwanziger (2009), 0904.2380.
 [34] M. Q. Huber, R. Alkofer, and S. P. Sorella (2009), 0910.5604.
 [35] R. Alkofer and L. von Smekal, Phys. Rept. **353**, 281 (2001), hep-ph/0007355.
 [36] C. S. Fischer, J. Phys. **G32**, R253 (2006), hep-ph/0605173.
 [37] D. Zwanziger, Phys. Rev. **D65**, 094039 (2002), hep-th/0109224.
 [38] D. Zwanziger, Phys. Rev. **D67**, 105001 (2003), hep-th/0206053.
 [39] J. M. Pawłowski, D. F. Litim, S. Nedelko, and L. von Smekal, Phys. Rev. Lett. **93**, 152002 (2004), hep-th/0312324.
 [40] C. S. Fischer and H. Gies, JHEP **10**, 048 (2004), hep-ph/0408089.
 [41] D. F. Litim and J. M. Pawłowski (1998), hep-th/9901063.
 [42] J. M. Pawłowski, Annals Phys. **322**, 2831 (2007), hep-th/0512261.
 [43] H. Gies (2006), hep-ph/0611146.
 [44] C. S. Fischer and J. M. Pawłowski, Phys. Rev. **D75**, 025012 (2007), hep-th/0609009.
 [45] C. S. Fischer and J. M. Pawłowski, Phys. Rev. **D80**, 025023 (2009), 0903.2193.
 [46] R. Alkofer, M. Q. Huber, and K. Schwenzer (2008), 0801.2762.
 [47] J. M. Pawłowski and L. von Smekal, work in preparation.
 [48] P. Boucaud et al., JHEP **06**, 001 (2006), hep-ph/0604056.
 [49] P. Boucaud et al., JHEP **06**, 012 (2008), 0801.2721.
 [50] P. Boucaud et al., JHEP **06**, 099 (2008), 0803.2161.
 [51] D. Dudal, S. P. Sorella, N. Vandersickel, and H. Verschelde, Phys. Rev. **D77**, 071501 (2008), 0711.4496.
 [52] D. Dudal, J. A. Gracey, S. P. Sorella, N. Vandersickel, and H. Verschelde, Phys. Rev. **D78**, 065047 (2008),

- 0806.4348.
- [53] S. P. Sorella, Phys. Rev. **D80**, 025013 (2009), 0905.1010.
- [54] D. Dudal, N. Vandersickel, H. Verschelde, and S. P. Sorella (2009), 0911.0082.
- [55] A. C. Aguilar and A. A. Natale, JHEP **08**, 057 (2004), hep-ph/0408254.
- [56] A. C. Aguilar and J. Papavassiliou, Phys. Rev. **D77**, 125022 (2008), 0712.0780.
- [57] D. Binosi and J. Papavassiliou, Phys. Rev. **D77**, 061702 (2008), 0712.2707.
- [58] A. C. Aguilar, D. Binosi, and J. Papavassiliou, Phys. Rev. **D78**, 025010 (2008), 0802.1870.
- [59] J. M. Cornwall, Phys. Rev. **D26**, 1453 (1982).
- [60] C. S. Fischer, A. Maas, and J. M. Pawłowski, PoS **CONFINEMENT8**, 043 (2008), 0812.2745.
- [61] K.-I. Kondo, Phys. Lett. **B678**, 322 (2009), 0904.4897.
- [62] K.-I. Kondo (2009), 0907.3249.
- [63] K.-I. Kondo (2009), 0909.4866.
- [64] K.-I. Kondo (2009), 0911.2880.
- [65] J. C. Taylor, Nucl. Phys. **B33**, 436 (1971).
- [66] A. Cucchieri, T. Mendes, and A. Mihara, JHEP **12**, 012 (2004), hep-lat/0408034.
- [67] J. C. R. Bloch, A. Cucchieri, K. Langfeld, and T. Mendes, Nucl. Phys. **B687**, 76 (2004), hep-lat/0312036.
- [68] W. Schleifenbaum, A. Maas, J. Wambach, and R. Alkofer, Phys. Rev. **D72**, 014017 (2005), hep-ph/0411052.
- [69] L. von Smekal, D. Mehta, A. Sternbeck, and A. G. Williams, PoS **LAT2007**, 382 (2007), 0710.2410.
- [70] L. von Smekal, M. Ghiotti, and A. G. Williams, Phys. Rev. **D78**, 085016 (2008), 0807.0480.
- [71] A. Cucchieri, T. Mendes, and A. R. Taurines, Phys. Rev. **D71**, 051902 (2005), hep-lat/0406020.
- [72] A. Sternbeck, E. M. Ilgenfritz, M. Muller-Preussker, A. Schiller, and I. L. Bogolubsky, PoS **LAT2006**, 076 (2006), hep-lat/0610053.
- [73] P. O. Bowman et al., Phys. Rev. **D76**, 094505 (2007), hep-lat/0703022.
- [74] R. Alkofer, W. Detmold, C. S. Fischer, and P. Maris, Phys. Rev. **D70**, 014014 (2004), hep-ph/0309077.
- [75] A. Maas, Phys. Rev. **D75**, 116004 (2007), 0704.0722.
- [76] A. Cucchieri and T. Mendes, Phys. Rev. Lett. **100**, 241601 (2008), 0712.3517.
- [77] G. 't Hooft, Nucl. Phys. **B75**, 461 (1974).
- [78] A. Sternbeck, E. M. Ilgenfritz, M. Mueller-Preussker, and A. Schiller, Phys. Rev. **D72**, 014507 (2005), hep-lat/0506007.
- [79] E. M. Ilgenfritz, M. Muller-Preussker, A. Sternbeck, A. Schiller, and I. L. Bogolubsky, Braz. J. Phys. **37**, 193 (2007), hep-lat/0609043.
- [80] A. Cucchieri and T. Mendes, PoS **LAT2007**, 297 (2007), 0710.0412.
- [81] I. L. Bogolubsky, E. M. Ilgenfritz, M. Muller-Preussker, and A. Sternbeck, PoS **LAT2007**, 290 (2007), 0710.1968.
- [82] I. L. Bogolubsky et al. (2008), 0804.1250.
- [83] I. L. Bogolubsky, E. M. Ilgenfritz, M. Muller-Preussker, and A. Sternbeck, Phys. Lett. **B676**, 69 (2009), 0901.0736.
- [84] C. S. Fischer, A. Maas, J. M. Pawłowski, and L. von Smekal, Annals Phys. **322**, 2916 (2007), hep-ph/0701050.
- [85] O. Oliveira and P. J. Silva, Eur. Phys. J. **C62**, 525 (2009), 0705.0964.
- [86] O. Oliveira, P. J. Silva, E. M. Ilgenfritz, and A. Sternbeck, PoS **LAT2007**, 323 (2007), 0710.1424.
- [87] O. Oliveira and P. J. Silva, Phys. Rev. **D79**, 031501 (2009), 0809.0258.
- [88] O. Oliveira and P. J. Silva (2009), 0910.2897.
- [89] A. Cucchieri, T. Mendes, and A. R. Taurines, Phys. Rev. **D67**, 091502 (2003), hep-lat/0302022.
- [90] A. Maas, Phys. Rev. **D79**, 014505 (2009), 0808.3047.
- [91] A. Cucchieri, Phys. Lett. **B422**, 233 (1998), hep-lat/9709015.
- [92] A. Cucchieri and T. Mendes (2009), 0904.4033.
- [93] E. Marinari, C. Parrinello, and R. Ricci, Nucl. Phys. **B362**, 487 (1991).
- [94] F. Barahona, J. Phys. **A15**, 3241 (1982).
- [95] I. L. Bogolubsky et al., Phys. Rev. **D77**, 014504 (2008), 0707.3611.
- [96] I. L. Bogolubsky et al., PoS **LAT2007**, 318 (2007), 0710.3234.
- [97] V. G. Bornyakov, V. K. Mitrjushkin, and M. Muller-Preussker, Phys. Rev. **D79**, 074504 (2009), 0812.2761.
- [98] A. Cucchieri, T. Mendes, O. Oliveira, and P. J. Silva, Phys. Rev. **D76**, 114507 (2007), 0705.3367.
- [99] A. Sternbeck, L. von Smekal, D. B. Leinweber, and A. G. Williams, PoS **LAT2007**, 340 (2007), 0710.1982.
- [100] K. G. Wilson, Phys. Rev. **D10**, 2445 (1974).
- [101] P. de Forcrand and R. Gupta, Nucl. Phys. Proc. Suppl. **9**, 516 (1989).
- [102] M. Creutz, Phys. Rev. **D21**, 2308 (1980).
- [103] K. Langfeld (2003), hep-lat/0301007.
- [104] D. B. Leinweber, J. I. Skullerud, A. G. Williams, and C. Parrinello (UKQCD), Phys. Rev. **D60**, 094507 (1999), hep-lat/9811027.
- [105] H. G. Dosch and V. F. Muller, Fortschr. Phys. **27**, 547 (1979).
- [106] P. Boucaud et al., Phys. Rev. **D72**, 114503 (2005), hep-lat/0506031.
- [107] A. Cucchieri, Nucl. Phys. **B508**, 353 (1997), hep-lat/9705005.
- [108] A. Cucchieri and T. Mendes, Phys. Rev. **D78**, 094503 (2008), 0804.2371.
- [109] A. Sternbeck, E. M. Ilgenfritz, and M. Muller-Preussker, Phys. Rev. **D73**, 014502 (2006), hep-lat/0510109.
- [110] A. Sternbeck, E. M. Ilgenfritz, M. Muller-Preussker, and A. Schiller, Nucl. Phys. Proc. Suppl. **153**, 185 (2006), hep-lat/0511053.
- [111] G. Meurant and Z. Strakoš, Acta Numerica **15**, 471 (2006).
- [112] L. von Smekal, A. Jorkowski, D. Mehta, and A. Sternbeck, PoS **CONFINEMENT8**, 048 (2008), 0812.2992.